# Antiadhesion Therapy for Urinary Tract Infections—A Balanced PK/PD Profile Proved To Be Key for Success

Xiaohua Jiang,[†] Daniela Abgottspon,[†] Simon Kleeb,[†] Said Rabbani, Meike Scharenberg, Matthias Wittwer, Martina Haug, Oliver Schwardt, and Beat Ernst*

Institute of Molecular Pharmacy, University of Basel, Klingelbergstrasse 50, 4056 Basel, Switzerland

Ⓢ Supporting Information

ABSTRACT: The initial step for the successful establishment of urinary tract infections (UTIs), predominantly caused by uropathogenic *Escherichia coli*, is the adhesion of bacteria to urothelial cells. This attachment is mediated by FimH, a mannose-binding adhesin, which is expressed on the bacterial surface. To date, UTIs are mainly treated with antibiotics, leading to the ubiquitous problem of increasing resistance against most of the currently available antimicrobials. Therefore, new treatment strategies are urgently needed, avoiding selection pressure and thereby implying a reduced risk of resistance. Here, we present a new class of highly active antimicrobials, targeting the virulence factor FimH. When the most potent representative, an indolinylphenyl mannoside, was administered in a mouse model at the low dosage of 1 mg/kg (corresponding to approximately 25 μg/mouse), the minimal therapeutic concentration to prevent UTI was maintained for more than 8 h. In a treatment study, the colony-forming units in the bladder could be reduced by almost 4 orders of magnitude, comparable to the standard antibiotic treatment with ciprofloxacin (8 mg/kg, sc).
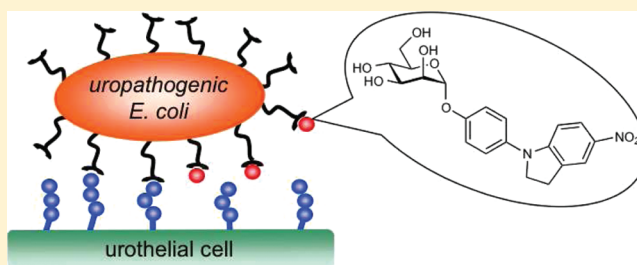
INTRODUCTION

Adhesion to target cells enables microorganisms to evade the natural clearing mechanisms and to ensure survival in the host environment. In urinary tract infections (UTIs), which are predominantly caused by uropathogenic *Escherichia coli* (UPEC), adhesion is accomplished by bacterial lectins, recognizing carbohydrate ligands located on the endothelial cells of the urinary tract.[1] For example, UPEC expressing P-pili cause pyelonephritis by binding to galabiose-containing ligands on the kidney epithelium, while mannose-binding type 1 piliated UPEC promote cystitis by targeting the glycoprotein uroplakin Ia (UPIa) on the mucosal surface of the urinary bladder. This initial step of the infection, the adhesion to the bacterial surface, prevents the rapid clearance of UPECs from the urinary tract by the bulk flow of urine and, at the same time, enables the invasion of host cells.[2,3] The most prevalent fimbriae encoded by UPEC consist of four subunits, FimA, FimF, FimG, and FimH.[4] The FimH lectin caps the fimbriae of type 1 pili and contains the carbohydrate recognition domain (CRD), mediating the crucial bacteria−cell interaction.[3]

UTIs affect a large proportion of the world population and account for significant morbidity and high medical costs.[2] Symptomatic UTIs should be treated with antibiotics to prevent potential devastating complications, like pyelonephritis and urosepsis. However, recurrent infections with subsequent antibiotic exposure can lead to emergence of antimicrobial resistance, which often results in treatment failure and reduces the range of therapeutic options. Hence, it is an urgent need for public health to develop an efficient, cost-effective, and nonantibiotic therapy to both prevent and treat UTIs without facilitating antimicrobial resistance.[5]

More than two decades ago, Sharon and co-workers have investigated various mannosides as antagonists for type 1 fimbriae-mediated bacterial adhesion.[6] For the further improvement of these FimH antagonists, two different approaches were explored. First, multivalent mannosides were investigated,[7,8] and second, monovalent high-affinity antagonists were designed (for representative examples, see Figure 1)[8] based on structural information obtained from crystal structures of the carbohydrate-recognition domain (CRD) of FimH cocrystallized with FimH antagonists.[9]

In this article, we present a new class of FimH antagonists. The binding affinities of these indolylphenyl and indolinylphenyl α-D-mannosides were determined in several target- and function-based assays. In addition, their in vitro pharmacokinetic properties were assigned, before the potential of selected compounds for in vivo application in a UTI mouse model was explored.

RESULTS AND DISCUSSION

Rational Design of FimH Antagonists. Crystal structures of FimH cocrystallized with various mannosides[9] disclosed a carbohydrate binding pocket with a hydrophobic entrance, the so-called tyrosine gate. The latter is formed by two tyrosines (Tyr48 and Tyr137) and an isoleucine (Ile52). Whereas *n*-butyl
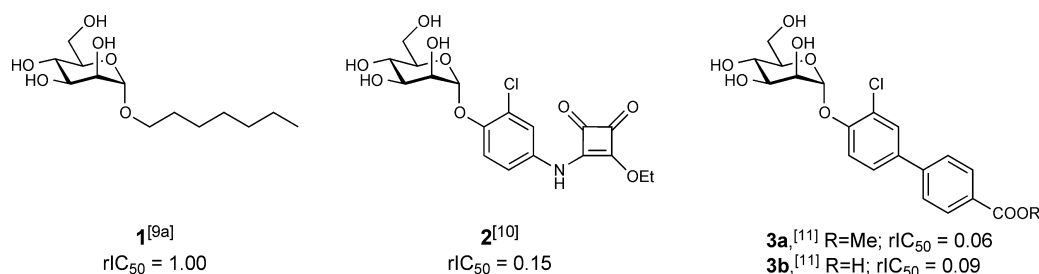
Figure 1. Alkyl (**1**) and aryl (**2** and **3**) α-D-mannopyranosides with nanomolar affinities. *n*-Heptyl α-D-mannoside (**1**) serves as a reference compound throughout our studies. Mannosides **2** and **3** exhibit low nanomolar affinities. Compound **3a** is the first reported orally available FimH antagonist that is hydrolyzed to the renally excretable acid **3b**. The IC_{50} values were determined with a cell-free binding assay.[12] Relative IC_{50} values (rIC_{50}) were calculated by dividing the IC_{50} of the substance of interest by the IC_{50} of the reference compound **1**.

α-D-mannoside populates the tyrosine gate and interacts with both tyrosines (in-docking mode),[9b,c] biphenyl α-D-mannosides, probably due to insufficient flexibility, adopt an out-docking mode, leading to an optimal π–π stacking of their outer aromatic ring with Tyr48.[9d] In several recent publications, biphenyl α-D-mannosides with excellent affinities were reported.[9d,11,13]

Here, antagonists with (aza)indolylphenyl and indolinyl-phenyl aglycones (see Table 1) are explored. According to our docking studies, the increased volume of the outer aromatic ring (indolyl/indolinyl vs phenyl) leads to an improved fit. Details are given in the Supporting Information.

Synthesis of FimH Antagonists. Starting from trichloro-acetimidate **5**, which was obtained from D-mannose (**4**) as reported earlier,[14] Lewis acid-promoted mannosylation of the phenols **6a–d** yielded the phenyl α-D-mannosides **7–10** (Scheme 1). In the subsequent copper-catalyzed Ullmann type coupling reaction[15] with the indoles **11e–j**, a partial deacetyla-tion of the mannose moiety was observed due to the use of K_2CO_3 or K_3PO_4 as a base. Therefore, the crude products were reacetylated to give the substituted 4-(indol-1-yl)phenyl α-D-mannopyranosides **12–20** and **30**. Saponification afforded the test compounds **21–29**, **31**, and **32** (Table 1).

Careful reduction of the nitro group in **13** by catalytic hydrogenation with PtO_2 in the presence of catalytic amounts of morpholine[16] quantitatively yielded the corresponding amine **33** (Scheme 2). Acylation with 4-chlorobenzoyl chloride or methanesulfonyl chloride (→ **34** and **35**) and subsequent deacetylation under Zemplén conditions gave the amides **36** and **37** (Table 1).

Starting from phenyl mannoside **7**, 7-azaindole derivatives **39** and **40** (Scheme 3) were obtained by an Ullmann type coupling reaction as well. Final deprotection yielded the test compounds **41** and **42** (Table 1).
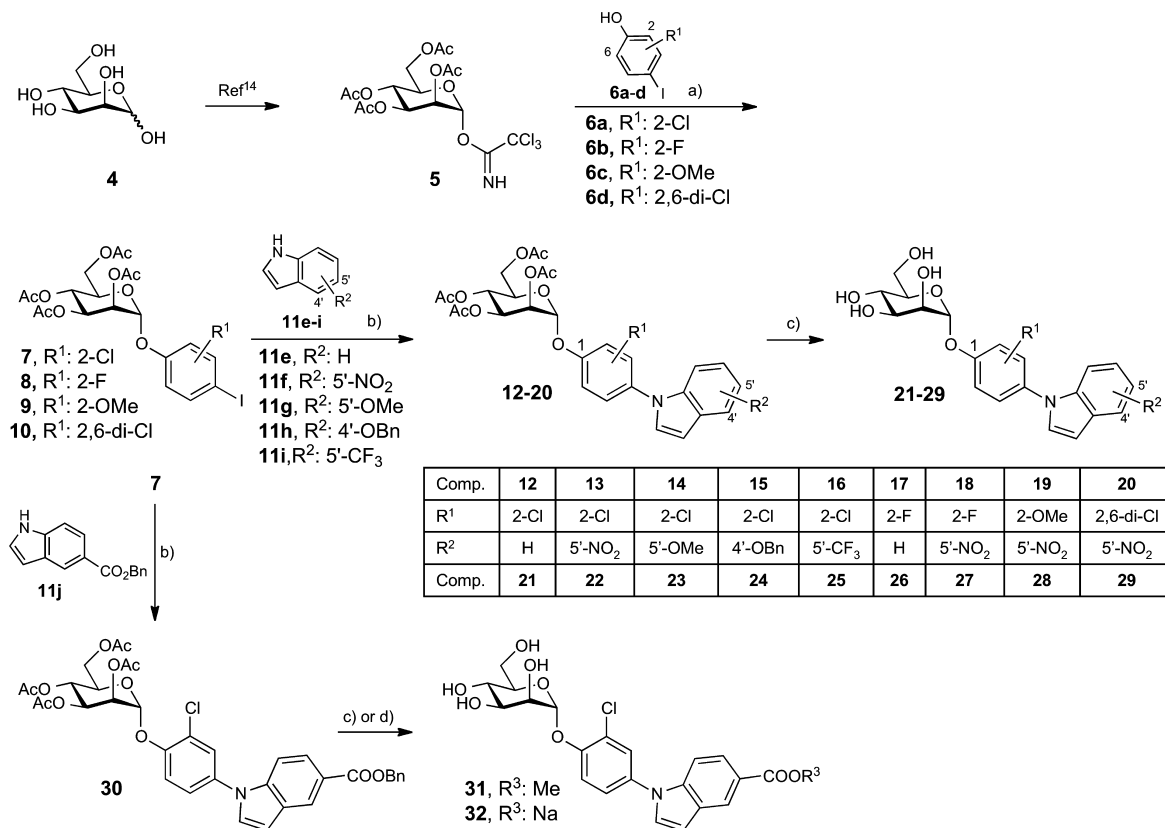
To further explore the contribution of the indole aglycone to binding, it was replaced by indoline moieties (→ **48a–d** and **52**, Scheme 4). The phenyl mannosides **44** and **50** were synthesized using the procedure as described for **7**. In a palladium-catalyzed Buchwald–Hartwig coupling[17] with 5-nitro-indoline (**45**) or indoline (**46**), the protected manno-sides **47a–d** and **51** were obtained in 43–80% yield. Final deacetylation under Zemplén conditions gave the indoline derivatives **48a–d** and **52** (Table 1).

Finally, the synthesis of the 5-linked 7-aza-indole **57** and the imidazo-pyridine derivative **58** is outlined in Scheme 5. Palladium-catalyzed Suzuki–Miyaura coupling[18] of **7** with boronic esters **53** or **54** (→ **55** and **56**) and subsequent deprotection afforded the test compounds **57** and **58** (Table 1).
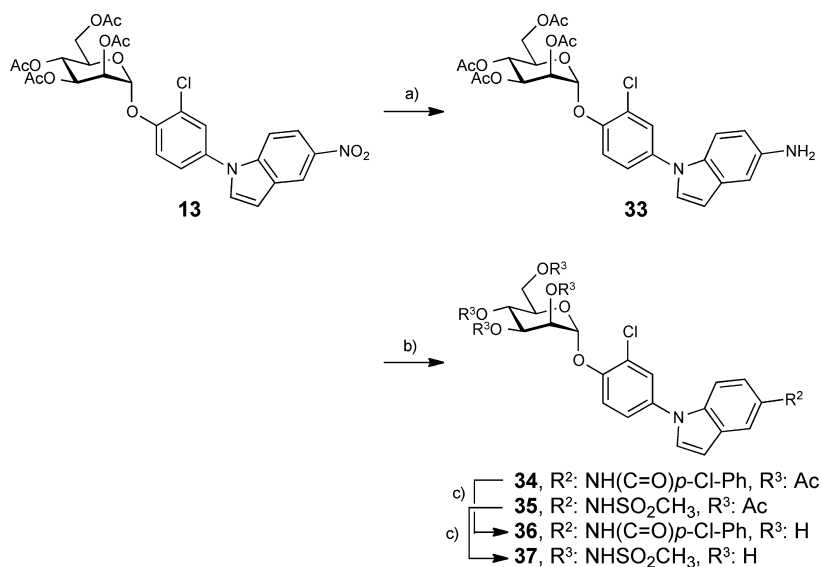
In Vitro Binding Affinities. To evaluate the potential of indolylphenyl and indolinylphenyl mannosides to prevent FimH-dependent adhesion of UPECs to urothelial cell surfaces, two different assay formats were applied. First, in the cell-free binding assay,[12] which is based on the interaction of a biotinylated polyacrylamide glycopolymer with the CRD of FimH, the inhibitory potency of FimH antagonists was measured. Second, in the cell-based aggregation assay,[19] the disaggregation of guinea pig erythrocytes (GPE) incubated with UPEC, strain UTI89 was determined as a function of various concentrations of FimH antagonists.

In the two assay formats, different affinities were expected. Whereas in the cell-free binding assay only the CRD of FimH is used, the complete pili are present in the cell-based aggregation assay. Furthermore, both formats are competitive assays, that is, the analyzed antagonists compete with mannosides for the binding site. In the cell-free binding assay, the competitor is a polymer-bound trimannoside, whereas in the aggregation assay, the antagonist competes with more potent oligo- and polysaccharide chains[20] present on the surface of erythro-cytes.[21] The interaction is further complicated by the existence of a high- and a low-affinity state of the CRD of FimH. Aprikian et al. experimentally demonstrated that in full-length fimbriae the pilin domain stabilizes the CRD domain in the low-affinity state, whereas the CRD domain alone adopts the high-affinity state.[22] Furthermore, it was recently shown that shear stress can induce a conformational switch (twist in the β-sandwich fold of the CRD domain) resulting in improved affinity.[23] Despite these differences, the ranking of the half maximal inhibitory concentration (IC_{50}) values within the two assay formats is expected to be in a similar order.

According to molecular dynamics (MD) simulations, a cavity between the *ortho*-hydrogen of the phenyl ring adjacent to the anomeric center and the binding pocket offers the opportunity to improve binding with a substituent of appropriate size, leading to refined van der Waals interactions. We therefore replaced the *ortho*-hydrogen by a chloro (entries 3–7 and 12–17), fluoro (entries 8 and 9), or methoxy substituent (entry 10). The *ortho*-chloro substituted antagonist showed the best binding affinities in both assays (Table 1). When a second chloro substituent was introduced to the *ortho'*-position (**29**, entry 11), the binding affinity unexpectedly decreased in both assays, indicating that the entropic gain expected by symmetrization of the antagonist could not be realized, probably because of rotational constraints. Therefore, an *ortho*-chloro substituent in the first aromatic ring was retained when the indole/indoline moiety was further optimized (**48a–d**, entries 18–21). As compared to the reference compound **1**, the indoline derivative **48c** (entry 20) exhibited an

Scheme 1[a]

Comp.	12	13	14	15	16	17	18	19	20
R[1]	2-Cl	2-Cl	2-Cl	2-Cl	2-Cl	2-F	2-F	2-OMe	2,6-di-Cl
R[2]	H	5'-NO$_2$	5'-OMe	4'-OBn	5'-CF$_3$	H	5'-NO$_2$	5'-NO$_2$	5'-NO$_2$
Comp.	21	22	23	24	25	26	27	28	29

[a]Reagents and conditions: (a) 4 Å MS, TMSOTf, toluene, rt, 2 h (37–94%). (b) (i) CuI, K$_2$CO$_3$, L-proline, DMSO, 90°C, overnight or CuI, K$_3$PO$_4$, *trans*-1,2-cyclohexanediamine, dioxane, 105°C, overnight; (ii) Ac$_2$O/pyr, DMAP, 2–4 h. (c) 0.5 M NaOMe/MeOH, rt. (d) 2N NaOH, THF/MeOH/H$_2$O (5:5:2), 40 °C (→ 32).

Scheme 2[a]

34, R[2]: NH(C=O)*p*-Cl-Ph, R[3]: Ac
35, R[2]: NHSO$_2$CH$_3$, R[3]: Ac
36, R[2]: NH(C=O)*p*-Cl-Ph, R[3]: H
37, R[3]: NHSO$_2$CH$_3$, R[3]: H

[a]Reagents and conditions: (a) H$_2$ (1 atm), PtO$_2$, cat. morpholine, MeOH/EtOAc (quant). (b) 4-Cl-BzCl or MeSO$_2$Cl, Et$_3$N, DCM, rt, 1 h (34, 94%; 35, 82%). (c) 0.5 M NaOMe/MeOH, rt (36, 85%; 37, 82%).

up to 30-fold improved affinity in the cell-free binding assay and the aggregometry assay. Finally, when the indolinyl substituent was introduced in the *meta*-positi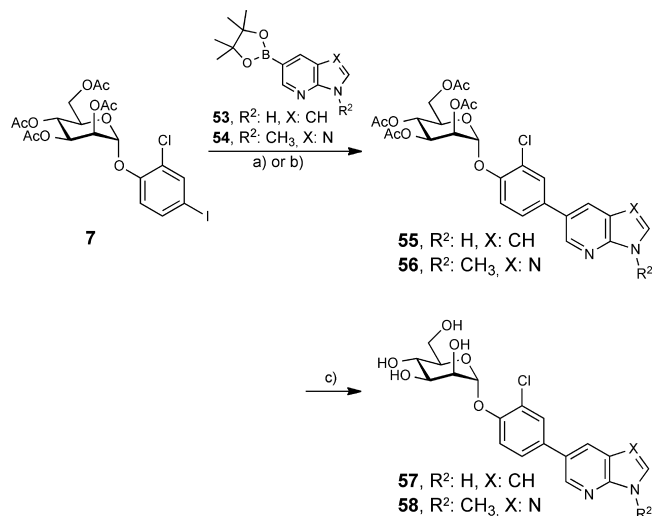on (→ 52, entry 22) or aza-indolyl (→ 57, entry 23) and imidazo-pyridyl substituents (→ 58, entry 24) were introduced in the *para*-position of the first aromatic ring, a substantial reduction in affinity was observed.

Scheme 3[a]

38k, R[2]: Cl
38l, R[2]: CN

39, R[2]: Cl, R[3]: Ac
40, R[2]: CN, R[3]: Ac
41, R[2]: Cl, R[3]: H
42, R[3]: CN, R[3]: H
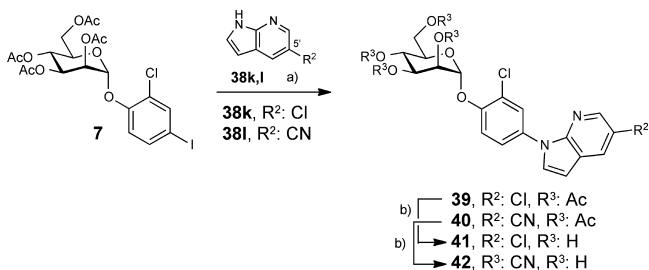
[a]Reagents and conditions: (a) (i) CuI, K$_2$CO$_3$, L-proline, DMSO, 90 °C, overnight or CuI, K$_3$PO$_4$, *trans*-1,2-cyclohexanediamine, dioxane, 105 °C, overnight; (ii) Ac$_2$O/pyr, DMAP, 2–4 h (**39**, 82%; **40**, 80%). (b) 0.5 M NaOMe/MeOH, rt (**41**, 63%; **42**, 91%).
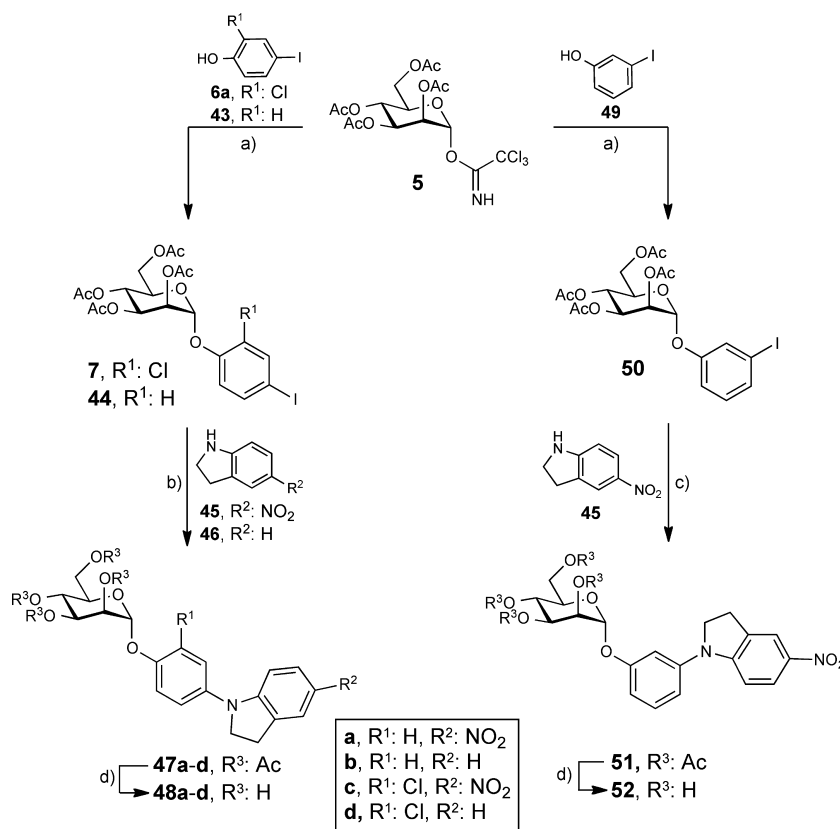
In Vitro Pharmacokinetic Characterization. To reach their therapeutic target, orally applied FimH antagonists should be gastrointestinally absorbed and renally eliminated; that is, an optimal balance between solubility, permeability, and lipophilicity is required. To identify the most promising candidates among the high-affinity FimH antagonists for the in vivo validation, membrane permeability, thermodynamic solubility, octanol–water partition, and plasma protein binding (PPB) were therefore determined.

The parallel artificial membrane permeability assay (PAMPA) predicts a medium to high oral absorption potential

Scheme 5[a]

53, R[2]: H, X: CH
54, R[2]: CH$_3$, X: N

55, R[2]: H, X: CH
56, R[2]: CH$_3$, X: N

57, R[2]: H, X: CH
58, R[2]: CH$_3$, X: N

[a]Reagents and conditions: (a) K$_3$PO$_4$, Pd(Ph$_3$P)$_4$, dioxane, 100 °C, overnight (**55**, 56%). (b) K$_3$PO$_4$, PdCl$_2$(dppf), DMF, 100 °C, overnight (**56**, 96%). (c) 0.5 M NaOMe/MeOH, rt, 2–2.5 h (**57**, 42%; **58**, 37%).

for compounds with an effective permeability (log P_e) above −6.3,[24] a property fulfilled by most of the listed indole and indoline derivatives (Table 2). Apparently, elevated lipophilicity of most antagonists, that is, log $D_{7.4} > 2$, facilitates permeation

Scheme 4[a]

6a, R[1]: Cl
43, R[1]: H

49

5

7, R[1]: Cl
44, R[1]: H

50

45, R[2]: NO$_2$
46, R[2]: H

45

a, R[1]: H, R[2]: NO$_2$
b, R[1]: H, R[2]: H
c, R[1]: Cl, R[2]: NO$_2$
d, R[1]: Cl, R[2]: H

47a-d, R[3]: Ac
48a-d, R[3]: H

51, R[3]: Ac
52, R[3]: H

[a]Reagents and conditions: (a) 4 Å MS, TMSOTf, toluene or DCM, rt, 2 h (**7**, 73%; **44**, quant; **50**, 93%). (b) Cs$_2$CO$_3$, Pd$_2$(dba)$_3$, X-Phos, toluene, 80 °C, 140 h or microwave, 80 °C, 8 h (**47a–d**, 43–75%). (c) Cs$_2$CO$_3$, Pd$_2$(dba)$_3$, X-Phos, dioxane, Ac$_2$O, pyr, 80 °C, 53 h (80%). (d) NaOMe/MeOH, rt, 20–23 h, (**48a–d**, 37–77%; **52**, 60%).

Table 1. In Vitro Pharmacodynamic Parameters of FimH Antagonists[a]

Entry	Comp. No.	R[1]	R[2]	X	Cell-free binding assay		Aggregometry assay	
					IC_{50} [nM]	rIC_{50}	IC_{50} [μM]	rIC_{50}
1	1[9a,11]		n-Heptyl α-D-mannopyranoside		73	1	77.1	1
2	3b[11]		Sodium 3'-chloro-4'-(α-D-manno-pyranosyloxy)-biphenyl-4-carboxylate		6.7	0.09	10.0	0.13

3	21	2-Cl	H	CH	14.9	0.2	8.3	0.11
4	22	2-Cl	5'-NO$_2$	CH	7.7	0.1	1.3	0.01
5	23	2-Cl	5'-OMe	CH	59.0	0.81	n.d.	-
6	24	2-Cl	4'-OBn	CH	48.6	0.66	n.a.	-
7	25	2-Cl	5'-CF$_3$	CH	18.8	0.26	6.4	0.08
8	26	2-F	H	CH	35.3	0.48	29.5	0.38
9	27	2-F	5'-NO$_2$	CH	52.8	0.72	5	0.06
10	28	2-OMe	5'-NO$_2$	CH	18.7	0.26	4.1	0.05
11	29	2,6-di-Cl	5'-NO$_2$	CH	28.1	0.38	7.1	0.09
12	31	2-Cl	5'-COOMe	CH	8.0	0.11	n.d.	-
13	32	2-Cl	5'-COOH	CH	20.3	0.28	3.1	0.04
14	36	2-Cl	5'-NH(C=O)pCl-Ph	CH	40.1	0.55	n.a.	-
15	37	2-Cl	5'-NHS(=O)$_2$Me	CH	20.7	0.28	5.6	0.07
16	41	2-Cl	5'-Cl	N	20.0	0.26	23.1	0.3
17	42	2-Cl	5'-CN	N	12.8	0.17	8.2	0.11

18	48a	H	NO$_2$	-	20	0.27	26.9	0.35
19	48b	H	H	-	14.5	0.20	n.d.	-
20	48c	Cl	NO$_2$	-	2.4	0.03	3.4	0.04
21	48d	Cl	H	-	27.8	0.43	n.d.	-

| 22 | 52 | | - | | 15.1 | 0.32 | 19.2 | 0.25 |

| 23 | 57 | - | H | CH | 40.1 | 0.55 | 35.9 | 0.47 |
| 24 | 58 | - | Me | N | 15.1 | 0.21 | 25.3 | 0.33 |

[a]The IC_{50} values were determined with the cell-free binding assay[12] and the aggregometry assay.[19] The rIC_{50} values were calculated by dividing the IC_{50} of the compound of interest by the IC_{50} of the reference compound 1. This leads to rIC_{50} values below 1 for derivatives binding better than 1 and rIC_{50} values above 1.00 for compounds with a lower affinity than 1. n.a., not active; n.d., not determined.

across the artificial membrane. In contrast to the promising PAMPA results, thermodynamic solubility strongly limited the dosages, which could be applied for the in vivo pharmacokinetic (PK) studies (see below).[25,26]

Regarding their renal elimination, lipophilic FimH antagonists (log $D_{7.4} > 2$) are expected to undergo considerable reabsorption in the renal tubules, leading overall only to a slow excretion into the bladder. On the contrary, hydrophilic

Table 2. Distribution Coefficients (log $D_{7.4}$ Values) Were Measured by a Miniaturized Shake Flask Procedure[29a]

entry	compd no.	log $D_{7.4}$	solubility/pH (μg/mL)	PAMPA log P_e (log 10^{-6} cm/s)	PPB (%)
25	3b[11]	−0.8	>3000	NP	89
26	21	1.8	31.5/6.5	−4.7	98
27	22	1.8	1.4/6.5	−4.9	99
28	23	3.0	9.6/6.6	−4.6	96
29	24	2.7	<0.1/6.5	NP	ND
30	25	ND	0.1/6.5	−4.6	>99
31	26	2.4	67/6.5	−4.7	98
32	27	1.9	4.0/6.5	−5.4	95
33	31	2.8	2.1/6.5	−4.4	99
34	32	1.1	1050/5.6	−6.4	93
35	36	ND	<0.001/6.5	−6	>99
36	37	1.8	279/6.3	NP	94
37	41	3.4	3.8/6.5	−5.0	96
38	42	1.6	8.5/6.3	−6.3	95
39	48a	1.9	24/6.5	−5.5	95
40	48b	2.3	31/6.5	−4.7	97
41	48c	1.9	3.6/6.5	−5.7	99
42	48d	2.8	21/6.5	−4.6	99
43	57	3.2	5.5/6.4	NP	90
44	58	1.3	2.4/6.3	−8.0	<30

[a]Thermodynamic solubility (S) was measured by an equilibrium shake flask approach.[30] Passive permeation through an artificial membrane and retention therein was determined by PAMPA.[24a] PPB was assessed following a miniaturized equilibrium dialysis protocol.[31] P_e, effective permeation; ND, not determined; NP, no permeation.

compounds (log $D_{7.4}$ < 0) are poorly reabsorbed and thus rapidly renally cleared, which leads to high initial compound levels in the urine but narrows the time range where a therapeutic concentration (T > MIC$_{adhesion}$, see below) is maintained.[27] Consequently, moderate lipophilicity, that is, log $D_{7.4}$ in the range of 1−2, is beneficial to maintain the drug concentration in the bladder over an extended time period. Most of the FimH antagonists listed in Table 2 show moderate to high lipophilicity and are therefore potentially affected by renal reabsorption. Moreover, PPB values ≥90% as found for most of the antagonists in Table 2 attenuate fast renal clearance, because, in line with the free drug hypothesis, molecules bound to plasma proteins evade excretion.[28] Compounds for the further evaluation were selected according to affinity (22 and 48c, Table 1) or their PK properties (21 and 48a, Table 2).

Determination of the Minimal Inhibitory Concentration of Adhesion (MIC$_{adhesion}$). Whereas in antimicrobial chemotherapy the MIC is defined as the lowest concentration of a drug that inhibits visible growth of an organism,[32] we defined a modified MIC for FimH antagonists because of their different mode of action (they neither kill nor inhibit the growth of bacteria). The MIC$_{adhesion}$ can be used for the determination of the therapeutic dosage in vivo and is defined as the concentration of antagonist leading to 90% inhibition of adhesion of the pathogen to the target cells (IC$_{90}$). To determine the MIC$_{adhesion}$, human bladder cells are infected with green fluorescent protein (GFP) labeled UPEC (strain UTI89) in the presence of different concentrations of FimH antagonists and analyzed by flow cytometry.[33] The half-maximal inhibitory concentration (IC$_{50}$) was calculated by plotting the mean fluorescent intensity (MFI) of the cells versus the concentration of the antagonist. From this plot, the concentration where 90% bacterial adhesion to human bladder cells is inhibited (IC$_{90}$) can

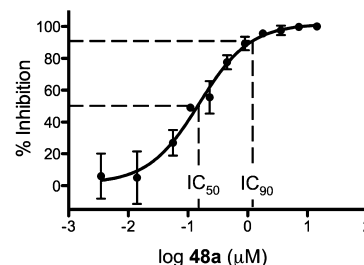| Entry	Comp. No.	IC$_{50}$ [μM]	IC$_{90}$ [μM]	MIC$_{Adhesion}$ [μg/mL]
45	3b	0.33 ± 0.05	1.4	0.61
46	21	20.14 ± 7.6	∼ 350	∼ 140
47	22	0.5 ± 0.29	2.9	1.32
48	48a	0.14 ± 0.05	1.16	0.49
49	48c	0.04 ± 0.02	0.3	0.14

Figure 2. Determination of the MIC$_{adhesion}$. The table lists the half-maximal inhibitory concentration (IC$_{50}$), the 90% inhibitory concentration of adhesion [IC$_{90}$ (μM)] and the MIC$_{adhesion}$ (μg/mL) of selected indolylphenyl (21 and 22) and indolinylphenyl (48a and 48c) mannosides as well as the previously reported biphenyl derivative 3b.[11] IC$_{50}$ values were determined using the cell-based flow cytometry infection assay[33] (see the graph, representing results for 48a). The MIC$_{adhesion}$ is the concentration in μg/mL of antagonist that inhibits adhesion of the pathogen to host cells by 90% (IC$_{90}$).

be deduced. The corresponding concentration in μg/mL was defined as MIC$_{adhesion}$. IC$_{50}$, IC$_{90}$, and MIC$_{adhesion}$ values of the four selected FimH antagonists and of the previously reported biphenyl derivative 3b[11] are listed in Figure 2.

Pharmacokinetic Studies in C3H/HeN Mice with a Single iv Dose. In our previously reported study,[11] FimH antagonist 3b was applied at a dosage of 50 mg/kg. For the in vivo characterization of the compounds of the new series, the dosage was adjusted according to their maximal solubility [in 5% aqueous dimethyl sulfoxide (DMSO)]. Plasma and urine concentrations of the selected FimH antagonists 3b,[11] 21, 22, 48a, and 48c after single iv application are summarized in Figure 3. The MIC$_{adhesion}$ values are indicated in the individual graphs with a dotted line. An important parameter for the prediction of the therapeutic outcome in the UTI mouse model is the time period for which the antagonist concentration in the urine is above the MIC$_{adhesion}$ (T > MIC$_{adhesion}$), representing the therapeutic time range.

As a consequence of fast renal excretion, the MIC$_{adhesion}$ value for reference compound 3b applied at a dosage of 50 mg/kg could be maintained for approximately 4 h (Figure 3A). When 21 and 22 were applied at dosages of 25 and 5 mg/kg, respectively, substantially lower urine concentrations were observed, for 21 below the MIC$_{adhesion}$ value and for 22 only marginally above (Figure 3B,C). Although compound 48a was applied with a single dose of 1 mg/kg (50-fold reduced dosage as compared to 3b), it exhibited the highest availability in the urine [area under the curve (AUC)$_{0-24}$] with a T > MIC$_{adhesion}$ of >8 h (Figure 3D). Finally, antagonist 48c was applied at 0.05 mg/kg, which is a 1000-fold reduced dosage as compared to 3b. Nevertheless, it still showed an improved therapeutic time range of 8 h (T > MIC$_{adhesion}$, Figure 3E).

Treatment Study in C3H/HeN Mice. For the in vivo UTI treatment study, antagonist 48a was selected for iv application (1 mg/kg) into the tail vein, followed by infection with UPEC (UTI89). The animals were sacrificed 3 h after inoculation, and

Antagonist Dosage	Compartment	$AUC_{0\text{-}24}$ [μg × h/mL]	$T > MIC_{Adhesion}$ [h]
3b 50 mg/kg	Plasma	20.8 ± 7.3	-
	Urine	209.6 ± 72.3	4
21 25 mg/kg	Plasma	8.2 ± 3.2	-
	Urine	19.3 ± 3.9	0
22 5 mg/kg	Plasma	2.3 ± 1.1	-
	Urine	13.2 ± 4.2	3
48a 1 mg/kg	Plasma	2.2 ± 0.8	-
	Urine	586.4 ± 251.6	> 8
48c 0.05 mg/kg	Plasma	3.5 ± 1.2	-
	Urine	33.4 ± 11	8
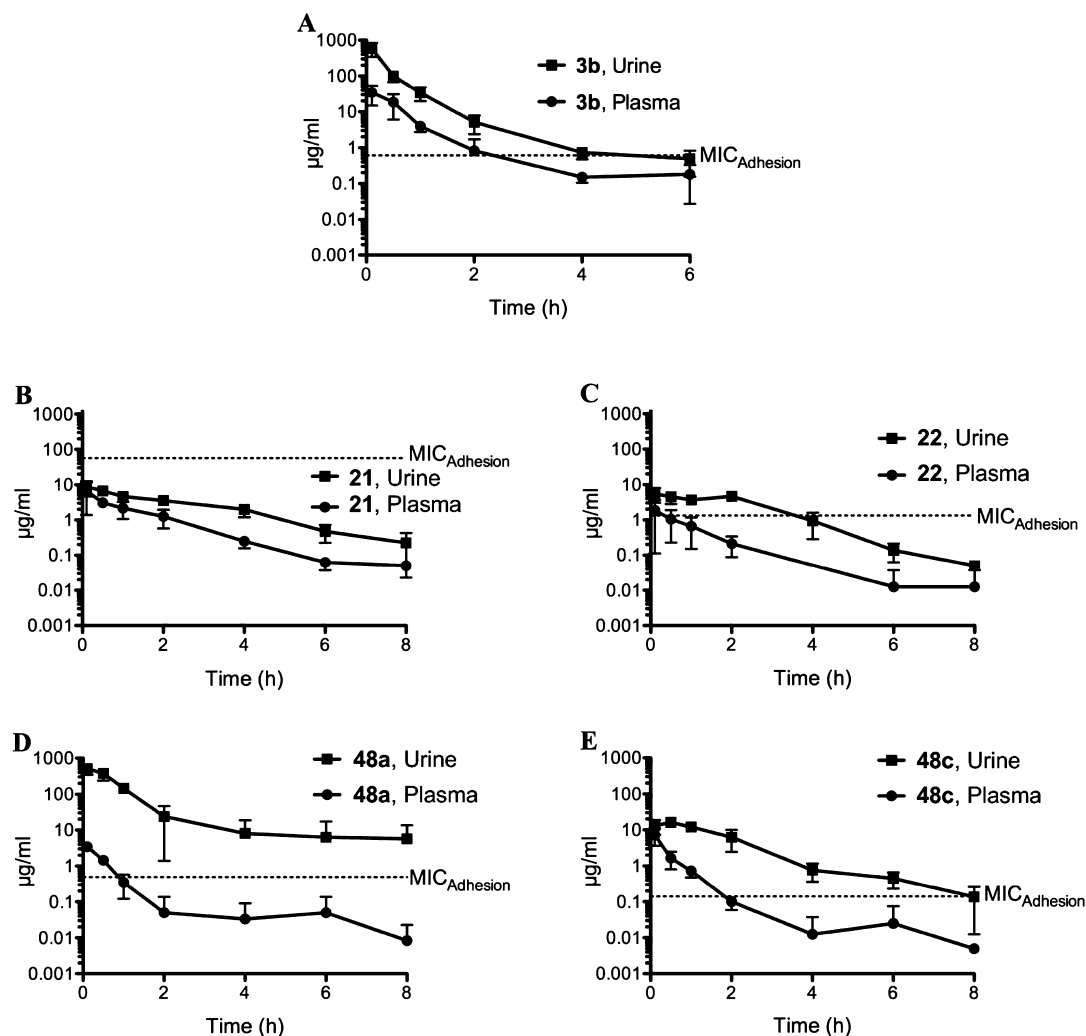
Figure 3. Determination of antagonist concentration in urine and plasma after a single iv application ($n = 4$). The data (table and graphs) show time-dependent urine and plasma concentrations and the $MIC_{adhesion}$ values as dotted lines for **3b** (reference compound[11]), **21**, **22**, **48a**, and **48c**. AUC_{0-24} is the AUC over 24 h; $MIC_{adhesion}$ is the minimal inhibitory concentration of adhesion.

homogenized organs (bladder and kidneys) were examined for bacterial counts. The results were compared to ciprofloxacin (CIP), used as standard antibiotic therapy against UTI.[34]

The mean value in the untreated control group showed bacterial counts of 1.4×10^8 colony-forming units (CFU) in the bladder and 9.7×10^6 CFU in the kidneys. The bar diagram in Figure 4 summarizes the bacterial counts after treatment. The baseline represents the values obtained for the control group, which was used as reference for CFU reductions. After iv application of **48a**, a substantial decrease of the bacterial counts

by $3.7 \log_{10}$ CFU was observed in the bladder. Results were compared to the previously presented antagonist **3b**,[11] which was tested using the same protocol. With **3b**, a 50-fold higher dosage (50 mg/kg) had to be applied to obtain a comparable reduction of $4 \log_{10}$ CFU for bladder counts. Mice treated with CIP (8 mg, sc) showed an almost identical reduction of bacterial counts in the bladder as the tested FimH antagonists **3b** (50 mg/kg) and **48a** (1 mg/kg). Furthermore, antagonist **48a** prevented bacteria from ascending into the kidneys ($-1.3 \log_{10}$ CFU) twice as efficiently as **3b** ($-0.7 \log_{10}$ CFU).
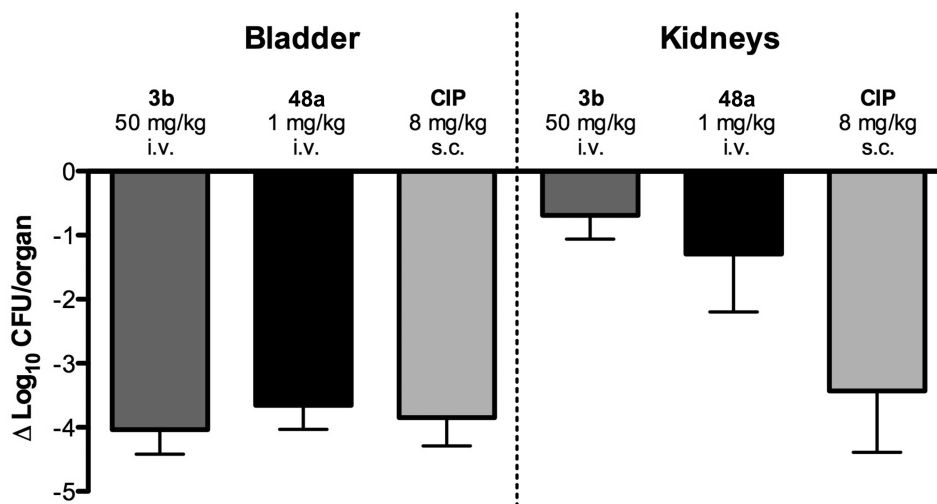
Figure 4. Treatment efficacy in the UTI mouse model 3 h after infection ($n = 6$). The bar diagram shows the reduction of bacterial counts of the indolinylphenyl mannoside **48a** at an iv dosage of 1 mg/kg, the biphenyl derivative **3b** at an iv dosage of 50 mg/kg, and ciprofloxacin (CIP) at an sc dosage of 8 mg/kg (representing the murine dose equivalent to a human standard dose).[35] The baseline represents the mean counts of the untreated control group; that is, the values of the control group were subtracted from the results of the tested antagonists.

As previously addressed,[11] urine samples show in general higher bacterial counts as compared to the bladder. A possible explanation is the varying urine volumes, leading to either a concentration or a dilution of bacteria in the urine samples. Therefore, results were limited to the evaluation of bladder and kidney counts. Furthermore, as compared to bladder counts, the bacterial counts in the kidneys were reduced to a smaller extent, probably due to different bacterial adhesion mechanisms in bladder and kidney (type 1 pili- vs P pili-dependent interactions).[3] Therefore, the considerable reduction of the bacterial counts in the kidney as observed for antagonist **48a** may originate from the inability of UPECs blocked by **48a** to adhere to bladder cells and their subsequent removal from the bladder by the urine flow. As a result, only a reduced population for ascending into the kidneys is available.

CONCLUSIONS

The FimH antagonists presented in this article exhibit an alternative mode of action as compared to antibiotics as they neither kill nor inhibit growth of bacteria. By blocking FimH, a lectin located at the tip of the bacterial fimbriae, they interfere with the adhesion of UPEC to the endothelial cells of the urinary tract and therewith the initial step of the infection. To select the most promising candidates for in vivo studies,[36] a thorough investigation of the in vitro potency and the physicochemical/PK properties of these FimH antagonists (Tables 1 and 2) was performed.

Starting from the known FimH antagonist biphenyl α-D-mannopyranoside (**3b**), we designed antagonists with spatially more demanding aglycones and therefore a better fit in the out-docking mode.[9d,13,37] Thus, a series of indolylphenyl and indolinylphenyl α-D-mannopyranosides were synthesized. For the initial evaluation of their affinities, a target-based, cell-free binding assay[12] and a cell-based aggregometry assay[19] were applied. In both series, an *ortho*-chloro substituent on the phenyl ring adjacent to the anomeric oxygen and an electron-withdrawing substituent on the indole/indoline moiety yielded the antagonists with the highest affinities/activities (see Table 1), presumably by favoring the π−π stacking with the electron rich Tyr48.

The most important requirement for a successful treatment in the UTI mouse model is the maintenance of a $MIC_{adhesion}$ of the antagonist in the urine. To avoid a fast renal clearance as experienced with the biphenyl mannoside **3b**[11] (log $D_{7.4}$ of −0.8, PPB 89%) (Figure 3A), the indole derivatives **21** and **22** and the indoline derivatives **48a** and **48c** exhibiting higher lipophilicity (log $D_{7.4}$ values of 1.8 and 1.9) and PPB (>95%) were selected as candidates for the in vivo PK study. Whereas for the indole derivatives **21** and **22** only insufficient urine concentrations (Figure 3B,C) were obtained, **48a** and **48c** exhibited a substantially improved renal elimination profile with $T > MIC_{adhesion}$ of >8 and 8 h, respectively, although 50−1000-fold lower dosages were applied (Figure 3D,E).

On the basis of these results, **48a** was selected for the treatment study in the UTI mouse model (dosage of 1 mg/kg). It reduced the CFUs in the bladder by 3.7 orders of magnitude, which is almost comparable to **3b**, applied at a 50-fold higher dosage (50 mg/kg, −4 $\log_{10}$ CFU). Furthermore, **48a** led to a considerably better reduction of bacterial counts in the kidneys (−1.3 $\log_{10}$ CFU vs −0.7 $\log_{10}$ CFU for **3b**). Of additional interest is the fact that the FimH antagonist **48a** was able to reduce bacterial infection in the bladder comparably well as the standard antibiotic treatment with ciprofloxacin (CIP),[34] indicating a promising profile for the alternative treatment of UTIs with FimH antagonists. Overall, the indoline derivative **48a** is the most active antagonist tested in vivo to date.[11,13] Because the experimental setup used in this study is a prophylactic approach, an adopted protocol for the treatment of an established infection is currently developed.

According to the PAMPA values, most representatives of the indole and indoline series are expected to be orally available (Table 2). However, a major drawback is their low solubility, limiting, for example, the dosage of **48a** to 1 mg/kg and **48c** to 0.05 mg/kg. To evaluate the dosage dependence, that is, whether higher dosages will further reduce the bacterial counts in bladder and kidney, the physicochemical issue of solubility will be addressed by appropriate formulations and structural modifications (e.g., by disruption of the molecular planarity of the aromatic aglycone[26]).

Overall, these results clearly indicate the high therapeutic potential of this new series of FimH antagonists. Because of optimized PK properties, a substantial reduction of the dosage could be achieved. Thus, with the most promising representative to date, the indolinylphenyl α-D-mannoside **48a**, the infection can be successfully treated with a low dosage of 1 mg/kg (approximately 25 μg/mouse) without any additional administration of antibiotics.

■ EXPERIMENTAL SECTION

Synthesis. The synthesis of compounds **7–10**, **14–20**, **23–37**, **39–42**, **44**, **47b,d**, **48b,d**, **50–52**, and **55–58**, including compound characterization data, can be found in the Supporting Information.

General Methods. Commercially available reagents were purchased from Fluka, Aldrich, Merck, AKSci, ASDI, or Alfa Aesar. Methanol (MeOH) was dried by distillation from sodium methoxide. Toluene and dioxane were dried by distillation from sodium/benzophenone. Optical rotations were measured at 20 °C on a Perkin-Elmer 341 polarimeter. Nuclear magnetic resonance (NMR) spectra were obtained on a Bruker Avance 500 UltraShield spectrometer at 500.13 MHz (^{1}H) or 125.76 MHz (^{13}C). Chemical shifts are given in ppm and were calibrated on residual solvent peaks or to tetramethylsilane as an internal standard. Multiplicities are specified as s (singlet), d (doublet), dd (doublet of a doublet), t (triplet), q (quartet), or m (multiplet). Assignment of the ^{1}H and ^{13}C NMR spectra was achieved using 2D methods (COSY, HSQC). ESI mass spectra were recorded on a Waters micromass ZQ instrument. High-resolution mass spectra were obtained on an ESI Bruker Daltonics micrOTOF spectrometer equipped with a TOF hexapole detector. Microwave-assisted reactions were carried out with CEM Discover and Explorer. Reactions were monitored by TLC using glass plates coated with silica gel 60 F$_{254}$ and visualized by using UV light and/or by charring with a molybdate solution (a 0.02 M solution of ammonium cerium sulfate dihydrate and ammonium molybdate tetrahydrate in aqueous 10% H$_2$SO$_4$) with heating to 150 °C for 5 min. Column chromatography was performed on a CombiFlash Companion (ISCO, Inc.) using RediSep normal phase disposable flash columns (silica gel). Reversed phase chromatography was performed on LiChroprepRP-18 (Merck, 40–63 μm).

Compound Purity. Each test compound was purified by chromatography on silica (dichloromethane (DCM)/MeOH, 10:1) or reversed-phase chromatography (RP-18 column, H$_2$O/MeOH, gradient from 0 to 20% MeOH), followed by Bio-Gel P2 (exclusion limit 1800 Da, Bio-Rad Laboratories) size exclusion chromatography (elution with water containing up to 20% MeOH at 0.25 mL/min) prior to HPLC, HRMS, NMR, and activity testing. The purity of all test compounds was determined by NMR and HPLC [Beckman Coulter Gold, consisting of pump 126, DAD 168 (190–410 nm), and autosampler 508. Column: Waters Atlantis T3, 3 μm, 2.1 mm × 100 mm. A, H$_2$O + 0.1% TFA; B, MeCN + 0.1% TFA. Detection, 270 nm. Gradient, 5 → 95% B (22 min); flow rate, 0.5 mL/min] to be ≥95% (for ^{1}H NMR spectra and HPLC traces, see the Supporting Information).

2-Chloro-4-(indol-1-yl)phenyl α-D-Mannopyranoside (21). A resealable Schlenk tube, which was equipped with a magnetic stirring bar, was charged with **7** (146 mg, 0.25 mmol), CuI (10 mg, 0.05 mmol), indole (**11e**, 35.0 mg, 0.30 mmol), K$_2$CO$_3$ (86 mg, 0.63 mmol), and L-proline (11.5 mg, 0.10 mmol). The vessel was sealed with a rubber septum, evacuated, and backfilled with argon (this process was repeated twice). Then, DMSO (1 mL) was added under a stream of argon, the reaction tube was quickly sealed, and the suspension was stirred at 90 °C overnight. The reaction mixture was cooled to rt, diluted with EtOAc (5 mL), and filtered through a plug of Celite. The filtrate was concentrated in vacuo, and the residue was treated for 2 h with Ac$_2$O/pyridine (3 mL, 1:2) and a catalytic amount of DMAP. The reaction was quenched by the addition of MeOH and concentrated, and the residue was purified by chromatography on silica (petroleum ether/EtOAc, 4:1 to 1:1) to give slightly impure **12** (40 mg, 28%). Compound **12** (40 mg, 0.07 mmol) was dissolved in MeOH (1 mL) and treated at rt with

0.5 M NaOMe/MeOH (14 μL) until completion of the reaction. The reaction mixture was neutralized with amberlyst-15 (H$^+$) ion-exchange resin and filtered. The filtrate was concentrated, and the residue was purified by chromatography on silica (DCM/MeOH, 10:1) and P2 size exclusion chromatography to afford **21** (20 mg, 70%) as a white solid after a final lyophilization from water/dioxane. $[\alpha]_D^{20}$ +171.6 (*c* 0.18, MeOH). ^{1}H NMR (500 MHz, CD$_3$OD): δ 7.62–7.54 (m, 3H, Ar–H), 7.45–7.38 (m, 3H, Ar–H), 7.18 (t, *J* = 7.0 Hz, 1H, Ar–H), 7.11 (t, *J* = 7.0 Hz, 1H, Ar–H), 6.65 (s, 1H, Ar–H), 5.61 (s, 1H, H-1), 4.14 (m, 1H, H-2), 4.01 (dd, *J* = 9.0, 2.5 Hz, 1H, H-3), 3.81–3.69 (m, 4H, H-6a, H-4, H-6b, H-5). ^{13}C NMR (125 MHz, CD$_3$OD): δ 151.81, 137.30, 136.22, 130.81, 128.98, 127.04, 125.58, 124.98, 123.49, 122.06, 121.42, 119.23, 111.00, 104.71 (Ar–C), 101.03 (C-1), 76.11 (C-5), 72.38 (C-3), 71.84 (C-2), 68.22 (C-4), 62.70 (C-6). HRMS (ESI) *m/z* calcd for C$_{20}$H$_{20}$ClNNaO$_6$ [M + Na]$^+$, 428.0877; found, 428.0875.

2-Chloro-4-(5-nitroindol-1-yl)phenyl α-D-Mannopyranoside (22). According to the procedure described for **21**, compound **22** was prepared from **7** (117 mg, 0.20 mmol) and 5-nitroindole (**11f**, 39 mg, 0.24 mmol) via the acetylated intermediate **13**. After workup, the residue was purified by chromatography on silica (DCM/MeOH, 10:1) and P2 size exclusion chromatography to yield **22** (54 mg, 60%) as a yellow solid after a final lyophilization from water/dioxane. $[\alpha]_D^{20}$ +85.7 (*c* 0.25, MeOH). ^{1}H NMR (500 MHz, CD$_3$OD): δ 8.63 (d, *J* = 2.0 Hz, 1H, Ar–H), 8.11 (dd, *J* = 9.0, 2.0 Hz, 1H, Ar–H), 7.65–7.55 (m, 4H, Ar–H), 7.48 (dd, *J* = 8.5, 2.5 Hz, 1H, Ar–H), 6.91 (d, *J* = 3.0 Hz, 1H, Ar–H), 5.65 (s, 1H, H-1), 4.14 (m, 1H, H-2), 4.01 (dd, *J* = 9.5, 3.5 Hz, 1H, H-3), 3.83–3.72 (m, 3H, H-6a, H-4, H-6b), 3.66 (m, 1H, H-5). ^{13}C NMR (125 MHz, CD$_3$OD): δ 152.73, 143.52, 140.14, 134.75, 132.99, 130.01, 127.65, 125.75, 125.57, 119.11, 118.95, 118.79, 111.51, 106.68 (Ar–C), 100.90 (C-1), 76.19 (C-5), 72.37 (C-3), 71.78 (C-2), 68.18 (C-4), 62.69 (C-6). HRMS (ESI) *m/z* calcd for C$_{20}$H$_{19}$ClN$_2$NaO$_8$ [M + Na]$^+$, 473.0728; found, 473.0728.

4-(5-Nitroindolin-1-yl)phenyl 2,3,4,6-Tetra-O-acetyl-α-D-manno-pyranoside (47a). In a Schlenk tube, a mixture of 2-dicyclohexyl-phosphino-2′,4′,6′-triisopropylbiphenyl (X-Phos) (9.1 mg, 0.019 mmol) and Pd$_2$(dba)$_3$ (3.85 mg, 0.0037 mmol) in dry toluene (3.5 mL) was stirred for 15 min at 40 °C under argon. Then, **44** (200 mg, 0.37 mmol), Cs$_2$CO$_3$ (364 mg 1.12 mmol), and 5-nitroindoline (**45**, 91.6 mg, 0.56 mmol) were added. The reaction mixture was degassed in an ultrasonic bath and stirred for 140 h at 80 °C. The reaction mixture was diluted with EtOAc (10 mL) and washed with aqueous saturated NaHCO$_3$ and brine. The aqueous layers were extracted with EtOAc (3 × 10 mL), and the combined organic layers were dried over Na$_2$SO$_4$, filtered, and concentrated under reduced pressure. The residue was purified by chromatography on silica (5–40% gradient of EtOAc in petrol ether) to give **47a** (163 mg, 75%) as an orange solid. $[\alpha]_D^{20}$ +55.0 (*c* 1.00, CHCl$_3$). ^{1}H NMR (500 MHz, CDCl$_3$): δ 7.98 (dd, *J* = 2.3, 8.9 Hz, 1H, Ar–H), 7.95 (s, 1H, Ar–H), 7.21 (m, 1H, Ar–H), 7.13 (m, 3H, Ar–H), 6.73 (d, *J* = 8.9 Hz, 1H, Ar–H), 5.55 (dd, *J* = 10.1, 3.5 Hz, 1H, H-3), 5.50 (d, *J* = 1.6 Hz, 1H, H-1), 5.44 (dd, *J* = 3.5, 1.8 Hz, 1H, H-2), 5.38 (t, *J* = 10.1 Hz, 1H, H-4), 4.28 (dd, *J* = 12.5, 5.2 Hz, 1H, H-6a), 4.08 (m, 4H, CH$_2$, H-6b, H-5), 3.19 (t, *J* = 8.6 Hz, 2H, CH$_2$), 2.20, 2.18, 2.04, 2.02 (4s, 12H, OAc). ^{13}C NMR (125 MHz, CDCl$_3$): δ 170.70, 170.23, 170.19, 169.90 (4 CO), 137.21, 128.40, 126.27, 122.03, 121.32, 117.92, 117.81, 105.52 (Ar–C), 96.36 (C-1), 69.53 (C-5), 69.40 (C-2), 68.98 (C-3), 66.03 (C-4), 62.28 (C-6), 53.85 (CH$_2$), 27.27 (CH$_2$), 21.65, 21.09, 20.92, 20.90 (4 COCH$_3$). MS (ESI) *m/z* calcd for C$_{28}$H$_{31}$N$_2$O$_{12}$ [M + H]$^+$, 587.19; found, 587.29.

2-Chloro-4-(5-nitroindolin-1-yl)phenyl 2,3,4,6-Tetra-O-acetyl-α-D-mannopyranoside (47c). According to the procedure described for **47a**, compound **7** (60 mg, 0.10 mmol) was microwave irradiated with Cs$_2$CO$_3$ (100 mg 0.30 mmol), X-Phos (4.9 mg, 0.010 mmol), Pd$_2$(dba)$_3$ (2.21 mg, 0.0020 mmol), and 5-nitroindoline (**45**, 50.5 mg, 0.30 mmol) in toluene (1 mL) to yield **47c** (36 mg, 56%) as an orange solid. $[\alpha]_D^{20}$ +99.6 (*c* 0.08, CHCl$_3$). ^{1}H NMR (500 MHz, CDCl$_3$): δ 8.03 (dd, *J* = 8.8, 2.3 Hz, 1H, Ar–H), 7.99 (m, 1H, Ar–H), 7.30 (d, *J* = 2.7 Hz, 1H, Ar–H), 7.26–7.08 (m, 2H, Ar–H), 6.82 (d, *J* = 8.9 Hz, 1H, Ar–H), 5.59 (dd, *J* = 10.1, 3.4 Hz, 1H, H-3), 5.54–5.46 (m, 2H, H-2, H-1), 5.39 (t, *J* = 10.1 Hz, 1H, H-4), 4.28 (dd, *J* = 12.2, 5.1 Hz, 1H, H-6a), 4.21 (m, 1H, H-5), 4.10 (dd, *J* = 12.3, 2.2 Hz,

1H, H-6b), 4.06 (t, J = 9.0 Hz, 2H, CH$_2$), 3.20 (t, J = 8.6 Hz, 2H, CH$_2$), 2.19, 2.06, 2.05, 2.03 (4s, 12H, OAc). ^{13}C NMR (125 MHz, CDCl$_3$): δ 170.69, 170.21, 170.04, 169.94 (4 CO), 152.91, 147.91, 138.24, 131.61, 129.24, 128.43, 125.72, 122.33, 121.42, 119.52, 118.45, 106.00 (Ar–C), 97.42 (C-1), 70.00 (C-3), 69.53 (C-2), 68.90 (C-5), 65.99 (C-4), 62.31 (C-6), 53.70 (CH$_2$), 27.31 (CH$_2$), 21.11, 20.94, 20.92 (4C, 4 COCH$_3$). MS (ESI) m/z calcd for C$_{28}$H$_{29}$ClN$_2$NaO$_{12}$ [M + Na]$^+$, 643.13; found, 643.19.

4-(5-Nitroindolin-1-yl)phenyl α-D-Mannopyranoside (48a). Compound **47a** (218 mg, 0.37 mmol) was dissolved in MeOH (2 mL) and treated at rt with 0.5 M NaOMe/MeOH (1 mL) for 20 h. The reaction mixture was neutralized with amberlyst-15 (H$^+$) ion-exchange resin and filtered. The filtrate was concentrated, and the residue was purified by RP-18 chromatography (H$_2$O/MeOH, gradient from 0 to 20% MeOH), followed by P2 size exclusion chromatography to yield **48a** (77.7 mg, 50%) as a colorless solid after a final lyophilization from water/dioxane. [α]$_D^{20}$ +57.0 (*c* 0.10, MeOH). ^{1}H NMR (500 MHz, CD$_3$OD): δ 8.00 (m, 2H, Ar–H), 7.31 (m, 2H, Ar–H), 7.21 (m, 2H, Ar–H), 6.78 (d, J = 8.5 Hz, 1H, Ar–H), 5.47 (d, J = 2.0 Hz, 1H, H-1), 4.12 (m, 2H, NCH$_2$), 4.02 (dd, J = 3.3, 1.8 Hz, 1H, H-2), 3.90 (dd, J = 9.4, 3.4 Hz, 1H, H-3), 3.79 (dd, J = 12.0, 6.4 Hz, 1H, H-6a), 3.73 (m, 2H, H-6b, H-4), 3.62 (ddd, J = 9.7, 5.3, 2.3 Hz, 1H, H-5), 3.21 (t, J = 8.5 Hz, 2H, CH$_2$). ^{13}C NMR (125 MHz, CD$_3$OD): δ 154.98, 137.95, 127.14, 123.52, 122.02, 119.08, 106.41 (Ar–C), 100.69 (C-1), 75.62 (C-5), 72.54 (C-3), 72.13 (C-2), 68.50 (C-4), 62.86 (C-6), 55.07 (CH$_2$), 28.03 (CH$_2$). HRMS (ESI) m/z calcd for C$_{20}$H$_{23}$N$_2$O$_8$ [M + H]$^+$, 419.1449; found, 419.1453.

2-Chloro-4-(5-nitroindolin-1-yl)phenyl α-D-Mannopyranoside (48c). According to the procedure described for **48a**, compound **47c** (36 mg, 0.058 mmol) was treated with 0.5 M NaOMe/MeOH (0.5 mL) in MeOH (1 mL) for 21 h. After workup, the residue was purified by RP-18 chromatography (H$_2$O/MeOH, gradient from 0 to 20% MeOH) and P2 size exclusion chromatography to yield **48c** (16.5 mg, 63%) as a colorless solid after a final lyophilization from water/dioxane. [α]$_D^{20}$ +53.8 (*c* 0.21, MeOH/CHCl$_3$). ^{1}H NMR (500 MHz, CD$_3$OD): δ 8.05–8.01 (m, 2H, Ar–H), 7.42 (m, 2H, Ar–H), 7.28 (dd, J = 9.0, 2.5 Hz, 1H, Ar–H), 6.86 (d, J = 8.5 Hz, 1H, Ar–H), 5.51 (d, J = 1.5 Hz, 1H, H-1), 4.11 (m, 3H, NCH$_2$, H-2), 3.97 (dd, J = 9.3, 3.4 Hz, 1H, H-3), 3.81(dd, J = 11.7, 2.2 Hz, 1H, H-6a), 3.64 (ddd, J = 9.7, 5.6, 2.2 Hz, 1H, H-5), 3.23 (t, J = 8.6 Hz, 2H, CH$_2$). ^{13}C NMR (125 MHz, CD$_3$OD): δ 134.69, 133.05, 132.87, 130.67, 129.03, 126.83, 123.31, 121.97, 121.31, 119.65, 106.72 (Ar–C), 101.25 (C-1), 76.04 (C-5), 72.40 (C-3), 71.88 (C-2), 68.27 (C-4), 62.73 (C-6), 54.74 (CH$_2$), 27.93 (CH$_2$). HRMS (ESI) m/z calcd for C$_{20}$H$_{21}$ClN$_2$NaO$_8$ [M + Na]$^+$, 475.0879; found, 475.0875.

In Vitro Activity. *Cell-Free Binding Assay.* To determine the affinity of the various FimH antagonists, a cell-free binding assay described previously[12] was applied. A recombinant protein consisting of the CRD of FimH linked with a thrombin cleavage site to a 6His-tag (FimH-CRD-Th-6His) was expressed in *E. coli* strain HM125 and purified by affinity chromatography. Microtiter plates (F96 MaxiSorp, Nunc) were coated with 100 μL/well of a 10 μg/mL solution of FimH-CRD-Th-6His in 20 mM HEPES, 150 mM NaCl, and 1 mM CaCl$_2$, pH 7.4 (assay buffer), overnight at 4 °C. The coating solution was discarded, and the wells were blocked with 150 μL/well of 3% BSA in assay buffer for 2 h at 4 °C. After three washing steps with assay buffer (150 μL/well), a 4-fold serial dilution of the test compound (50 μL/well) in assay buffer containing 5% DMSO and streptavidin-peroxidase coupled biotinylated polyacrylamide (PAA) glycopolymers [Manα1–3(Manα1–6)Manβ1–4GlcNAcβ1–4GlcNAcβ-PAA-biotin, TM-PAA] (50 μL/well of a 0.5 μg/mL solution), was added. On each individual microtiter plate, *n*-heptyl α-D-mannopyranoside (**1**) was tested as a reference compound. The plates were incubated for 3 h at 25 °C and 350 rpm and then carefully washed four times with 150 μL/well assay buffer. After the addition of 100 μL/well of the horseradish peroxidase substrate 2,2′-azino-di(3-ethylbenz-thiazoline-6-sulfonic acid) (ABTS), the colorimetric reaction was allowed to develop for 4 min, then stopped by the addition

of 2% aqueous oxalic acid before the optical density (OD) was measured at 415 nm on a microplate-reader (Spectramax 190, Molecular Devices, CA). The IC$_{50}$ values of the compounds tested in duplicates were calculated with the prism software (GraphPad Software, Inc., La Jolla, CA). The IC$_{50}$ defines the molar concentration of the test compound that reduces the maximal specific binding of TM-PAA polymer to FimH-CRD by 50%. The relative IC$_{50}$ (rIC$_{50}$) is the ratio of the IC$_{50}$ of the test compound to the IC$_{50}$ of *n*-heptyl α-D-mannopyranoside (**1**).

Bacteria and Growth. The clinical *E. coli* isolate UTI89[38] (UTI89wt) was kindly provided by the group of Prof. Urs Jenal, Biocenter, University of Basel, Switzerland. Microorganisms were stored at −70 °C and incubated for 24 h before the experiments under static conditions at 37 °C in 10 mL of Luria–Bertani broth (Becton, Dickinson and Company, Le Pont de Claix, France) using 50 mL tubes. Prior to each experiment, the microorganisms were washed twice and resuspended in phosphate-buffered saline (PBS, Sigma-Aldrich, Buchs, Switzerland). Bacterial concentrations were determined by plating serial 1:10 dilutions on blood agar, followed by colony counting with 20–200 colonies after overnight incubation at 37 °C.

Aggregometry Assay. The aggregometry assay was carried out as previously described.[19] In short, the percentage of aggregation of *E. coli* UTI89 with GPEs was quantitatively determined by measuring the optical density at 740 nm and 37 °C under stirring at 1000 rpm using an APACT 4004 aggregometer (Endotell AG, Allschwil, Switzerland). Bacteria were cultivated as described above. GPEs were separated from guinea pig blood (Charles River Laboratories, Sulzfeld, Germany) using Histopaque (density of 1.077 g/mL at 24 °C, Sigma-Aldrich). Prior to the measurements, the cell densities of *E. coli* and GPE were adjusted to an OD$_{600}$ of 4, corresponding to 1.9 × 10^8 CFU/mL and 2.2 × 10^6 cells/mL, respectively. For the calibration of the instrument, the aggregation of platelet poor plasma (PPP) using PBS alone was set as 100%, and the aggregation of platelet rich plasma (PRP) using GPE was set as 0%. After calibration, measurements were performed with 250 μL of GPE and 50 μL of bacterial suspension, and the aggregation was monitored over 600 s. After the aggregation phase of 600 s, 25 μL of antagonist in PBS was added to each cuvette, and disaggregation was monitored for 1400 s.

Cultivation of 5637 Cells. The human epithelial bladder carcinoma cell line 5637 was obtained from the German Collection of Microorganisms and Cell Cultures (DSMZ, Braunschweig, Germany). The cells were grown in RPMI 1640 medium, supplemented with 10% fetal calf serum (FCS), 100 U/mL penicillin, and 100 μg/mL streptomycin at 37 °C, 5% CO$_2$. All solutions were purchased from Invitrogen (Basel, Switzerland). The cells were subcultured 1:5 twice per week for six passages before using them in the infection assay. Two days before infection, 1.8 × 10^5 cells were seeded in each well of a 24-well plate in RPMI 1640 containing 10% FCS without antibiotics. The cell density was approximately (3−5) × 10^5 cells/well prior the infection.

Flow Cytometry Infection Assay. The infection assay was carried out as previously described.[33] Briefly, to evaluate FimH antagonists, a serial dilution of the antagonists in 5% DMSO was prepared. Before infection, a suspension of green fluorescently labeled (GFP) bacteria (UTI89, 200 μL) and 25 μL of the test compound were preincubated for 10 min at room temperature. The bacteria–antagonist mixture was then added to the monolayer of 5637 cells (grown in 24-well plates, as described above) at a multiplicity of infection (MOI) of 1:50 (cell:bacteria). To homogenize the infection, plates were centrifuged at room temperature for 3 min at 600g. After an incubation of 1.5 h at 37 °C, infected cells were washed four times with RPMI 1640 medium and suspended in ice-cold PBS for 5−20 min. Cells were then kept in the dark until analysis. All measurements were made within 1 h after the termination of the infection. Samples were acquired in a CyAn ADP flow cytometer (Becton, Dickinson and Company) and analyzed by gating on the eukaryotic cells based on forward (FSC) and side scatter (SSC), which excludes unbound GFP-labeled bacteria and debris from analysis. A total of 10^4 cells were measured per sample. Data were acquired in a linear mode for the side scatter (SSC) and in a logarithmic mode for the forward scatter (FSC) and the green

fluorescent channel FL1-H (e.g., GFP). The MFI of FL1-H was counted as a surrogate marker for the adherence of bacteria. Quantification of adhesion was evaluated with the FlowJo software 9.0.1 (Tree Star, Inc., Ashland, OR). IC_{50} values were determined by plotting the concentration of the antagonist in logarithmic mode versus the MFI and by fitting the curve with the prism software (GraphPad, inhibition curve, nonlinear regression, variable slope, $n = 4$). The IC_{90} ($F = 90$) was calculated from the determined IC_{50} value and the hill slope (H) as follows:

$$IC_F = \left(\frac{F}{100 - F}\right)^{1/H} \times IC_{50}$$

In Vitro Pharmacokinetic Parameters. *Materials.* DMSO and 1-octanol were purchased from Sigma-Aldrich. PAMPA System Solution, GIT-0 Lipid solution, and Acceptor Sink Buffer were ordered from pIon (Woburn, MA). Human plasma was bought from Biopredic (Rennes, France), and acetonitrile (MeCN) was from Acros Organics (Geel, Belgium).

Log $D_{7.4}$ Determination. The in silico prediction tool ALOGPS[39] was used to estimate the log P values of the compounds. Depending on these values, the compounds were classified into three categories: hydrophilic compounds (log P below zero), moderately lipophilic compounds (log P between zero and one), and lipophilic compounds (log P above one). For each category, two different ratios (volume of 1-octanol to volume of buffer) were defined as experimental parameters (Table 3).

Table 3

compd type	log P	ratios (1-octanol:buffer)
hydrophilic	<0	30:140, 40:130
moderately lipophilic	0−1	70:110, 110:70
lipophilic	>1	3:180, 4:180

Equal amounts of phosphate buffer (0.1 M, pH 7.4) and 1-octanol were mixed and shaken vigorously for 5 min to saturate the phases. The mixture was left until separation of the two phases occurred, and the buffer was retrieved. Stock solutions of the test compounds were diluted with buffer to a concentration of 1 μM. For each compound, six determinations, that is, three determinations per 1-octanol:buffer ratio, were performed in different wells of a 96-well plate. The respective volumes of buffer containing analyte (1 μM) were pipetted to the wells and covered by saturated 1-octanol according to the chosen volume ratio. The plate was sealed with aluminum foil, shaken (1350 rpm, 25 °C, 2 h) on a Heidolph Titramax 1000 plate-shaker (Heidolph Instruments GmbH & Co. KG, Schwabach, Germany), and centrifuged (2000 rpm, 25 °C, 5 min, 5804 R Eppendorf centrifuge, Hamburg, Germany). The aqueous phase was transferred to a 96-well plate for analysis by LC-MS (see below).

log $D_{7.4}$ was calculated from the 1-octanol:buffer ratio (o:b), the initial concentration of the analyte in buffer (1 μM), and the concentration of the analyte in the aqueous phase (c_B) with equation:

$$\log D_{7.4} = \log\left(\frac{1\,\mu M - c_B}{c_B} \times \frac{1}{o:b}\right)$$

The average of the three log $D_{7.4}$ values per 1-octanol:buffer ratio was calculated. If the two means obtained for a compound did not differ by more than 0.1 unit, the results were accepted.

PAMPA. Log P_e was determined in a 96-well format with the PAMPA[24a] permeation assay. For each compound, measurements were performed at three pH values (5.0, 6.2, and 7.4) in quadruplicates. For this purpose, 12 wells of a deep well plate, that is, four wells per pH value, were filled with 650 μL of System Solution. Samples (150 μL) were withdrawn from each well to determine the blank spectra by UV spectroscopy (SpectraMax 190, Molecular Devices). Then, analyte dissolved in DMSO was added to the remaining System Solution to yield 50 μM solutions. To exclude precipitation, the optical density was measured at 650 nm, with 0.01 being the threshold value. Solutions exceeding this threshold were filtrated. Afterward, samples (150 μL) were withdrawn to determine the reference spectra. Further samples (200 μL) were transferred to each well of the donor plate of the PAMPA sandwich (pIon, Woburn, MA, P/N 110 163). The filter membranes at the bottom of the acceptor plate were impregnated with 5 μL of GIT-0 Lipid Solution, and 200 μL of Acceptor Sink Buffer was filled into each acceptor well. The sandwich was assembled, placed in the GutBox, and left undisturbed for 16 h. Then, it was disassembled, and samples (150 μL) were transferred from each donor and acceptor well to UV plates. Quantification was performed by both UV spectroscopy and LC-MS (see below). log P_e values were calculated with the aid of the PAMPA Explorer Software (pIon, version 3.5).

Thermodynamic Solubility. Microanalysis tubes (LaboTech J. Stofer LTS AG, Muttenz, Switzerland) were charged with 1 mg of solid substance and 250 μL of phosphate buffer (50 mM, pH 6.5). The tubes were briefly shaken by hand, sonicated for 15 min, and vigorously shaken (600 rpm, 25 °C, 2 h) on an Eppendorf Thermomixer Comfort. Afterward, they were left undisturbed for 24 h. After the pH was measured, the compound solutions were filtered (MultiScreen HTS 96-well Filtration System, Millipore, Billerica, MA) by centrifugation (1500 rpm, 25 °C, 3 min). The filtrates were diluted (1:2, 1:10, and 1:100 or, if the results were outside of the calibration range, 1:1000 and 1:10000), and the concentrations were determined by LC-MS (see below). The calibration was based on six values ranging from 0.1 to 10 μg/mL.

PPB. The dialysis membranes (MWCO 12−14 K; HTDialysis LCC, Gales Ferry, CT) were prepared according to the instructions of the manufacturer. The human plasma was centrifuged (5800 rpm, 25 °C, 10 min), the pH of the supernatant (without floating plasma lipids) was adjusted to 7.5, and the analyte was added to yield 10 μM solutions. PPB determinations were performed in triplicate. Equal volumes (150 μL) of phosphate buffer (0.1 M, pH 7.4) and plasma containing the analyte were transferred to the separated compartments of the 96-well high throughput dialysis block (HTDialysis LCC). The plate was covered with a sealing film and incubated (5 h, 37 °C). Afterward, samples (90 μL) were withdrawn from the buffer compartments and diluted with plasma (10 μL). From the plasma compartments, samples (10 μL) were withdrawn and diluted with phosphate buffer (90 μL). The solutions were further diluted with ice-cooled MeCN (300 μL) to precipitate the proteins and centrifuged (3600 rpm, 4 °C, 11 min). The supernatants (50 μL) were retrieved, and the analyte concentrations were determined by LC-MS (see below). The fraction bound (f_b) was calculated as follows:

$$f_b = 1 - \frac{c_b}{c_p}$$

where c_b is the concentration of the analyte in the buffer compartment and c_p is the concentration in the plasma compartment. The values were accepted if the recovery of analyte was between 80 and 120% of the initial amount.

LC-MS Measurements. Analyses were performed using a 1100/1200 Series HPLC System coupled to a 6410 Triple Quadrupole mass detector (Agilent Technologies, Inc., Santa Clara, CA) equipped with electrospray ionization. The system was controlled with the Agilent MassHunter Workstation Data Acquisition software (version B.01.04). The column used was an Atlantis T3 C18 column (2.1 mm × 50 mm) with a 3 μm particle size (Waters Corp., Milford, MA). The mobile phase consisted of two eluents: solvent A (H_2O, containing 0.1% formic acid, v/v) and solvent B (acetonitrile, containing 0.1% formic acid, v/v), both delivered at a flow rate of 0.6 mL/min. The gradient was ramped from 95% A/5% B to 5% A/95% B over 1 min and then held at 5% A/95% B for 0.1 min. The system was then brought back to 95% A/5% B, resulting in a total duration of 4 min. MS parameters such as fragmentor voltage, collision energy, and polarity were optimized individually for each compound, and the molecular ion was followed for each compound in the multiple reaction monitoring

mode. The concentration of each analyte was quantified by the Agilent Mass Hunter Quantitative Analysis software (version B.01.04).

In Vivo Pharmacokinetic and Treatment Studies. *Animals.* Female C3H/HeN mice weighing between 19 and 25 g were obtained from Charles River Laboratories and were housed three or four to a cage. Mice were kept under specific pathogen-free conditions in the Animal House of the Department of Biomedicine, University Hospital Basel, and animal experimentation guidelines according to the regulations of Swiss veterinary law were followed. After 7 days of acclimatization, 9−10 week old mice were used for the PK and infection study. During the studies, animals were allowed free access to chow and water. Three days before infection studies and during infection, 5% D-(+)-glucose (AppliChem, Baden-Dättwil, Switzerland) was added to the drinking water, to increase the number of bacterial counts in the urine and kidneys.[40]

Pharmacokinetic Studies. Single-dose PK studies were performed by iv application of the FimH antagonist at the designated dosages followed by urine and plasma sampling. For iv application, the antagonists were diluted in 100 μL of PBS and injected into the tail vein. Blood and urine were sampled (10 μL) after 6 and 30 min and 1, 2, 4, 6, and 8 h. Before analysis, proteins in blood and urine samples were precipitated using methanol (Acros Organics) and centrifuged for 11 min at 13000 rpm. The supernatant was transferred into a 96-well plate (0.5 mL, polypropylene, Agilent Technologies) and analyzed by LC-MS as described above.

UTI Mouse Model. Mice were infected as previously described.[40] In brief, before infection, all remaining urine was depleted form the bladder by gentle pressure on the abdomen. Mice were anesthetized with 1.1 vol% isoflurane/oxygen mixture (Attane, Minrad Inc., Buffalo, NY) and placed on their backs. Anesthetized mice were inoculated transurethrally with the bacterial suspension by use of a 2 cm polyethylene catheter (Intramedic polyethylene tubing; inner diameter, 0.28 mm; outer diameter, 0.61 mm; Beckton, Dickinson and Company), which was placed on a syringe (Hamilton Gastight Syringe 50 μL, removable 30G needle, BGB Analytik AG, Boeckten, Switzerland). The catheter was gently inserted through the urethra until it reached the top of the bladder, followed by slow injection of 50 μL of bacterial suspension at a concentration of approximately 5×10^7 to 5×10^8 CFU.

Antagonist Treatment Studies. The FimH antagonists were applied iv in 100 μL of PBS into the tail vein 10 min before infection. Three hours after the onset of infection, mice were sacrificed with CO_2. Organs were removed aseptically and homogenized in 1 mL of PBS by using a tissue lyser (Retsch, Haan, Germany). Serial dilutions of bladder and kidneys were plated on Levine Eosin Methylene Blue Agar plates (Beckton, Dickinson and Company). CFU counts were determined after overnight incubation at 37 °C and expressed as CFU/organ, corresponding to CFU/bladder and CFU/2 kidneys.

ASSOCIATED CONTENT

Ⓢ Supporting Information

Synthesis of compounds **7−10, 14−20, 23−37, 39−42, 44, 47b,d, 48b,d, 50−52,** and **55−58**; HRMS data, HPLC traces, and ^{1}H NMR spectra for the target compounds **21−29, 31, 32, 36, 37, 41, 42, 48a−d, 52, 57,** and **58**. This material is available free of charge via the Internet at http://pubs.acs.org.

AUTHOR INFORMATION

Corresponding Author
*Tel: +41 61 267 15 51. Fax: +41 61 267 15 52. E-mail: beat. ernst@unibas.ch.

Author Contributions
[†]These authors contributed equally to the project.

Notes
The authors declare no competing financial interest.

ABBREVIATIONS USED

ABTS, 2,2′-azino-di(3-ethylbenzthiazoline-6-sulfonic acid); AUC, area under the curve; CFU, colony-forming units; CRD, carbohydrate recognition domain; log $D_{7.4}$, distribution coefficient at pH 7.4; DCM, dichloromethane; dba, dibenzylideneacetone; DMSO, dimethyl sulfoxide; GFP, green fluorescent protein; GPE, guinea pig erythrocytes; IC_{50}, half maximal inhibitory concentration; IC_{90}, concentration where 90% of the maximal observed effect is obtained; iv, intravenous; $MIC_{adhesion}$, minimal inhibitory concentration of adhesion; Man, D-mannose; MD, molecular dynamics; MFI, mean fluorescent intensity; NMR, nuclear magnetic resonance; PAMPA, parallel artificial membrane permeation assay; P_e, effective permeation; PPB, plasma protein binding; PK, pharmacokinetic; PPP, platelet poor plasma; PRP, platelet rich plasma; rIC_{50}, relative inhibitory concentration; S, solubility; SAR, structure−activity relationship; sc, subcutaneous; $T > MIC_{adhesion}$, time over the minimal inhibitory concentration of adhesion; TM-PAA, Manα1−3(Manα1−6)Manβ1−4GlcNAcβ1−4GlcNAcβ-polyacrylamide-biotin; TMSOTf, trimethylsilyl trifluoromethanesulfonate; UPEC, uropathogenic *Escherichia coli*; UPIa, uroplakin Ia; UTI, urinary tract infection; X-Phos, 2-dicyclohexylphosphino-2′,4′,6′-triisopropylbiphenyl

REFERENCES

(1) (a) Berglund, J.; Knight, S. D. Structural basis for bacterial adhesion in the urinary tract. *Adv. Exp. Med. Biol.* **2003**, *535*, 33−52. (b) Westerlund-Wikström, B.; Korhonen, T. K. Molecular structure of adhesin domains in *Escherichia coli* fimbriae. *Int. J. Med. Microbiol.* **2005**, *295*, 479−486.

(2) Wiles, T. J.; Kulesus, R. R.; Mulvey, M. A. Origins and virulence mechanisms of uropathogenic *Escherichia coli*. *Exp. Mol. Pathol.* **2008**, *85*, 11−19.

(3) Mulvey, M. A. Adhesion and entry of uropathogenic *Escherichia coli*. *Cell Microbiol.* **2002**, *4*, 257−271.

(4) Capitani, G.; Eidam, O.; Glockshuber, R.; Grutter, M. G. Structural and functional insights into the assembly of type 1 pili from *Escherichia coli*. *Microbes Infect.* **2006**, *8*, 2284−2290.

(5) Sharon, N. Carbohydrates as future anti-adhesin drugs for infectious diseases. *Biochim. Biophys. Acta* **2006**, *1760*, 527−537.

(6) (a) Firon, N.; Ofek, I.; Sharon, N. Interaction of mannose-containing oligosaccharides with the fimbrial lectin of *Escherichia coli*. *Biochem. Biophys. Res. Commun.* **1982**, *105*, 1426−1432. (b) Firon, N.; Ofek, I.; Sharon, N. Carbohydrate specificity of the surface lectins of *Escherichia coli*, *Klebsiella pneumoniae* and *Salmonella typhimurium*. *Carbohydr. Res.* **1983**, *120*, 235−249. (c) Sharon, N. Bacterial lectins, cell-cell recognition and infectious disease. *FEBS Lett.* **1987**, *217*, 145−157.

(7) (a) Pieters, R. J. Maximising multivalency effects in protein-carbohydrate interactions. *Org. Biomol. Chem.* **2009**, *7*, 2013−2025. (b) Imberty, A.; Chabre, Y. M.; Roy, R. Glycomimetics and glycodendrimers as high affinity microbial anti-adhesins. *Chem.—Eur. J.* **2008**, *14*, 7490−7499.

(8) Hartmann, M.; Lindhorst, T. K. The bacterial lectin FimH, a target for drug discovery-carbohydrate inhibitors of type 1 fimbriae-mediated bacterial adhesin. *Eur. J. Org. Chem.* **2011**, 3583−3609.

(9) (a) Choudhury, D.; Thompson, A.; Stojanoff, V.; Langermann, S.; Pinkner, J.; Hultgren, S. J.; Knight, S. D. X-ray structure of the FimC-FimH chaperone-adhesin complex from uropathogenic *Escherichia coli. Science* **1999**, *285*, 1061−1066. (b) Bouckaert, J.; Berglund, J.; Schembri, M.; Genst, E. D.; Cools, L.; Wuhrer, M.; Hung, C. S.; Pinkner, J.; Slättergard, R.; Zavialov, A.; Choudhury, D.; Langermann, S.; Hultgren, S. J.; Wyns, L.; Klemm, P.; Oscarson, S.; Knight, S. D.; Greve, H. D. Receptor binding studies disclose a novel class of high-affinity inhibitors of the *Escherichia coli* FimH adhesin. *Mol. Microbiol.* **2005**, *55*, 441−455. (c) Wellens, A.; Garofalo, C.; Nguyen, H.; Van Gerven, N.; Slättergârd, R.; Hernalsteens, J.-P.; Wyns, L.; Oscarson, S.; De Greve, H.; Hultgren, S.; Bouckaert, J. Intervening with urinary tract infections using anti-adhesives based on the crystal structure of the FimH-oligomannose-3 complex. *PLos One* **2008**, *3*, 4−13. (d) Han, Z.; Pinker, J. S.; Ford, B.; Obermann, R.; Nolan, W.; Wildman, S. A.; Hobbs, D.; Ellenberger, T.; Cusumano, C. K.; Hultgren, S. J.; Janetka, J. W. Structure-based drug design and optimization of mannoside bacterial FimH antagonists. *J. Med. Chem.* **2010**, *53*, 4779−4792.

(10) (a) Sperling, O.; Fuchs, A.; Lindhorst, T. K. Evaluation of the carbohydrate recognition domain of the bacterial adhesin FimH: design, synthesis and binding properties of mannoside ligands. *Org. Biomol. Chem.* **2006**, *4*, 3913−3922. (b) Grabosch, C.; Hartmann, M.; Schmidt-Lassen, J.; Lindhorst, T. K. Squaric acid monoamide mannosides as ligands for the bacterial lectin FimH: Covalent inhibition or not? *ChemBioChem* **2011**, *12*, 1066−1074.

(11) Klein, T.; Abgottspon, D.; Wittwer, M.; Rabbani, S.; Herold, J.; Jiang, X.; Kleeb, S.; Lüthi, C.; Scharenberg, M.; Bezençon, J.; Gubler, E.; Pang, L.; Smiesko, M.; Cutting, B.; Schwardt, O.; Ernst, B. FimH antagonist for the oral treatment of urinary tract infections: From design and synthesis to in vitro and in vivo evaluation. *J. Med. Chem.* **2010**, *53*, 8627−8641.

(12) Rabbani, S.; Jiang, X.; Schwardt, O.; Ernst, B. Expression of the carbohydrate recognition domain of FimH and development of a competitive binding assay. *Anal. Biochem.* **2010**, *407*, 188−195.

(13) Cusumano, C. K.; Pinkner, J. S.; Han, Z.; Greene, S. E.; Ford, B. A.; Crowley, J. R.; Henderson, J. P.; Janetka, J. W.; Hultgren, S. J. Treatment and prevention of urinary tract infection with orally active FimH inhibitors. *Sci. Transl. Med.* **2011**, *3*, 1−10.

(14) Kerékgyártó, J.; Kamerling, J. P.; Bouwstra, J. B.; Vliegenthasrt, J. F. G.; Liptak, A. Synthesis of four structural elements of xylose-containing carbohydrate chains from N-glycoproteins. *Carbohydr. Res.* **1989**, *186*, 51−62.

(15) (a) Ma, D.; Cai, Q. L-Proline promoted Ullmann type coupling reactions of aryl iodides with indoles, pyrroles, imidazoles or pyrazoles. *Synlett* **2004**, 128−130. (b) Ma, D.; Cai, Q. Copper/Amino acid catalyzed cross-couplings of aryl and vinyl halides with nucleophiles. *Acc. Chem. Res.* **2008**, *41*, 1450−1460. and the references thereof (c) Ley, S. V.; Thomas, A. W. Modern Synthetic methods for copper-mediated C(aryl)-O, C(aryl)-N, and C(aryl)-S bond formation. *Angew. Chem., Int. Ed.* **2003**, *42*, 5400−5449. (d) Antilla, J. C.; Klapars, A.; Buchwald, S. L. The copper-catalyzed N-arylation of indoles. *J. Am. Chem. Soc.* **2002**, *124*, 11684−11688.

(16) Kosak, J. R. Catalytic hydrogenation of aromatic halonitro compounds. *Ann. N.Y. Acad. Sci.* **1970**, *172*, 175−185.

(17) Wolfe, J. P.; Wagaw, S.; Marcoux, J.-F.; Buchwald, S. L. Rational development of practical catalysts for aromatic carbon-nitrogen bond formation. *Acc. Chem. Res.* **1998**, *31*, 805−818.

(18) Prieto, M; Zurita, E.; Rosa, E.; Muñoz, L.; Lloyd-Williams, P.; Giralt, E. Arylboronic acids and arylpinacolboronate esters in Suzuki-coupling reactions involving indoles. Partner role swapping and heterocycle protection. *J. Org. Chem.* **2004**, *69*, 6812−6820.

(19) Abgottspon, D.; Rölli, G.; Hosch, L.; Steinhuber, A.; Jiang, X.; Schwardt, O.; Cutting, B.; Smiesko, M.; Jenal, U.; Ernst, B.; Trampuz, A. Development of an aggregation assay to screen FimH antagonists. *J. Microbiol. Methods* **2010**, *82*, 249−255.

(20) Bouckaert, J.; Mackenzie, J.; de Paz, J. L.; Chipwaza, B.; Choudhury, D.; Zavialov, A.; Mannerstedt, K.; Anderson, J.; Pierard, D.; Wyns, L.; Seeberger, P. H.; Oscarson, S.; De Greve, H.; Knight, S. D. The affinity of the FimH fimbrial adhesin is receptor-driven and quasi-independent of *Escherichia coli* pathotypes. *Mol. Microbiol.* **2006**, *61*, 1556−1568.

(21) Giampapa, C. S.; Abraham, S. N.; Chiang, T. M.; Beachey, E. H. Isolation and characterization of a receptor for type 1 fimbriae of *Escherichia coli* from guinea pig erythrocytes. *J. Biol. Chem.* **1988**, *263*, 5362−5367.

(22) Aprikian, P.; Tchesnokova, V.; Kidd, B.; Yakovenko, O.; Yarov-Yarovoy, V.; Trinchina, E.; Vogel, V.; Thomas, W.; Sokurenko, E. Interdomain interaction in the FimH adhesin of *Escherichia coli* regulates the affinity to mannose. *J. Biol. Chem.* **2007**, *282*, 23437−23446.

(23) Trong, I. L.; Aprikian, P.; Kidd, B. A.; Forero-Shelton, M.; Tchesnokova, V.; Rajagopal, P.; Rodriguez, V.; Interlandi, G.; Klevit, R.; Vogel, V.; Stenkamp, R. E.; Sokurenko, E. V.; Thomas, W. E. Structural basis for mechanical force regulation of the adhesin FimH via finger trap-like beta sheet twisting. *Cell* **2010**, *141*, 645−655.

(24) (a) Kansy, M.; Senner, F.; Gubernator, K. Physicochemical high throughput screening: Parallel artificial membrane permeation assay in the description of passive absorption processes. *J. Med. Chem.* **1998**, *41*, 1007−1010. (b) Avdeef, A.; Bendels, S.; Di, L.; Faller, B.; Kansy, M.; Sugano, K.; Yamauchi, Y. Parallel artificial membrane permeability assay (PAMPA)-critical factors for better predictions of absorption. *J. Pharm. Sci.* **2007**, *96*, 2893−2909.

(25) Lipinski, C. A. Drug-like properties and the causes of poor solubility and poor permeability. *J. Pharmacol. Toxicol. Methods* **2000**, *44*, 235−249.

(26) Lovering, F.; Bikker, J.; Humblet, C. Escape from flatland: increasing saturation as an approach to improving clinical success. *J. Med. Chem.* **2009**, *52*, 6752−6756.

(27) van de Waterbeemd, H.; Smith, D. A.; Beaumont, K.; Walker, D. K. Property-based design: optimization of drug absorption and pharmacokinetics. *J. Med. Chem.* **2001**, *44*, 1313−1333.

(28) (a) Schmidt, S.; Gonzalez, D.; Derendorf, H. Significance of protein binding in pharmacokinetics and pharmacodynamics. *J. Pharm. Sci.* **2010**, *99*, 1107−1122. (b) Trainor, G. L. The importance of plasma protein binding in drug discovery. *Expert Opin. Drug Discovery* **2007**, *2*, 51−64. (c) Weisiger, R. A. Dissociation from albumin: a potentially rate-limiting step in the clearance of substances by the liver. *Proc. Natl. Acad. Sci. U.S.A.* **1985**, *82*, 1563−1567.

(29) Dearden, J. C.; Bresnen, J. G. M. The measurement of partition coefficients. *QSAR Comb. Sci.* **1988**, *7*, 133−144.

(30) Kerns, E. H. High throughput physicochemical profiling for drug discovery. *J. Pharm. Sci.* **2001**, *90*, 1838−1858.

(31) Banker, M. J.; Clark, T. H.; Williams, J. A. Development and validation of a 96-well equilibrium dialysis apparatus for measuring plasma protein binding. *J. Pharm. Sci.* **2003**, *92*, 967−974.

(32) Andrews, J. M. Determination of minimum inhibitory concentrations. *J. Antimicrob. Chemother.* **2001**, *48* (Suppl1), 5−16.

(33) Scharenberg, M.; Abgottspon, D.; Ciceck, E.; Jiang, X.; Schwardt, O.; Rabbani, S.; Ernst, B. Flow cytometry-based assay for screening FimH antagonists. *Assay Drug Dev. Technol.* **2011**, *9*, 455−464.

(34) Hooton, T. M. Fluoroquinolones and resistance in the treatment of uncomplicated urinary tract infection. *Int. J. Antimicrob. Agents* **2003**, *22*, 65−72.

(35) Jakobsen, L.; Cattoir, V.; Hammerum, A. M.; Nordmann, P.; Frimodt-Møller, N. Impact of low-level fluoroquinolone resistance genes qnrA1, qnrB19, and qnrS1 on ciprofloxacin treatment of *Escherichia coli* urinary tract infection in murine model. Poster presented at ICAAC 2010. 50th Interscience Conference on Antimicrobial Agents and Chemotharapy, 2010, Sep 12−15, Boston, MA.

(36) (a) Russell, W. M. S.; Burch, R. L. *The Principles of Humane Experimental Technique*; Methuen: London, 1959; reprinted: Universities Federation for Animal Welfare, Wheathampstead, United

Kingdom, 1992. (b) Demers, G.; Griffin, G.; De Vroey, G.; Haywood, J. R.; Zurlo, J.; Bédard, M. Harmonization of animal care and use guidance. *Science* **2006**, *312*, 700−701.

(37) Schwardt, O.; Rabbani, S.; Hartmann, M.; Abgottspon, D.; Wittwer, M.; Kleeb, S.; Zalewski, A.; Smiesko, M.; Cutting, B.; Ernst, B. Design, Synthesis and biological evaluation of mannosyl triazoles as FimH antagonists. *Bioorg. Med. Chem.* **2011**, *19*, 6454−6473.

(38) Mulvey, M. A.; Schilling, J. D.; Hultgren, S. J. Establishment of a persistent *Escherichia coli* reservoir during the acute phase of a bladder infection. *Infect. Immun.* **2001**, *69*, 4572−4579.

(39) (a) VCCLAB, Virtual Computational Chemistry Laboratory; http://www.vcclab.org, 2005. (b) Tetko, I. V.; Gasteiger, J.; Todeschini, R.; Mauri, A.; Livingstone, D.; Ertl, P.; Palyulin, V. A.; Radchenko, E. V.; Zefirov, N. S.; Makarenko, A. S.; Tanchuk, V. Y.; Prokopenko, V. V. Virtual computational chemistry laboratory— Design and description. *J. Comput.-Aided Mol. Des.* **2005**, *19*, 453−463.

(40) Kerrn, M. B.; Frimodt-Møller, N.; Espersen, F. Effects of sulfomethizole and amdinocillin against *Escherichia coli* strains (with various susceptibilities) in an ascending urinary tract infection model. *Antimicrob. Agents Chemother.* **2003**, *47*, 1002−1009.